

# Monte Carlo modeling of spallation targets containing uranium and americium

Yury Malyshkin<sup>a</sup>, Igor Pshenichnov<sup>a,b</sup>, Igor Mishustin<sup>a,c</sup>, Walter Greiner<sup>a</sup>

<sup>a</sup>Frankfurt Institute for Advanced Studies, J.-W. Goethe University, 60438 Frankfurt am Main, Germany

<sup>b</sup>Institute for Nuclear Research, Russian Academy of Sciences, 117312 Moscow, Russia

<sup>c</sup>National Research Center "Kurchatov Institute", 123182 Moscow, Russia

---

## Abstract

Neutron production and transport in spallation targets made of uranium and americium are studied with a Geant4-based code MCADS (Monte Carlo model for Accelerator Driven Systems). A good agreement of MCADS results with experimental data on neutron- and proton-induced reactions on <sup>241</sup>Am and <sup>243</sup>Am nuclei allows to use this model for simulations with extended Am targets. Several geometry options and material compositions (U, U+Am, Am, Am<sub>2</sub>O<sub>3</sub>) are considered for spallation targets to be used in Accelerator Driven Systems. It was demonstrated that MCADS model can be reliably used for calculating critical masses of fissile materials. All considered options operate as deep subcritical targets having neutron multiplication factor of  $k \sim 0.5$ . It is found that more than 4 kg of Am can be burned in one spallation target during the first year of operation.

**Keywords:** spallation reactions, minor actinides, neutron sources, Accelerator Driven Systems, radioactive waste

---

## 1. Introduction

Many neutrons can be produced in spallation nuclear reactions [1, 2] induced by energetic protons in collisions with heavy target nuclei like W, Ta, Bi and Pb due to their enhanced neutron content with respect to lighter nuclei. This method to create an intense flux of neutrons is known for decades and it is already employed in several existing [3, 4] spallation neutron sources and will be used in the facilities to be constructed, e.g., in the ESS project [5]. Such facilities are dedicated to neutron imaging and scattering experiments [6]. Accelerator Driven Systems (ADS) aimed at energy production in subcritical assemblies of fissile materials or burning nuclear waste [7, 8] also use an intense proton beam to produce neutrons in spallation targets. The design of a spallation target is a challenging part of such projects in view of high energy deposited by the proton beam and secondary particles and the radi-

ation damage of the target material. The performance of a target irradiated by a megawatt-power proton beam was the subject of a dedicated experiment [9].

Heavy materials like W, Ta, Bi and Pb are commonly used in the design of spallation targets. Although the fission of such nuclei can, in principle, be induced by energetic protons [10], its role in neutron production is negligible. However, an alternative approach can be also considered to involve fissionable, <sup>232</sup>Th, <sup>238</sup>U [11], or even fissile, <sup>235</sup>U, <sup>242m</sup>Am [12], materials in the design of a spallation target. The difference between these two groups of materials consists in the capability of fissile material to sustain a nuclear chain reaction once a critical mass of this material is accumulated. Such materials can be either directly irradiated by a proton beam, or used as a blanket surrounding a non-fissionable material impacted by protons. In both cases neutron production is boosted due to additional fission neutrons. As recently demonstrated by our calculations [13], the number of neutrons produced per beam proton is about 3 times higher in a uranium target compared to one made of tung-

---

Email addresses: malyshkin@fias.uni-frankfurt.de (Yury Malyshkin), pshenich@fias.uni-frankfurt.de (Igor Pshenichnov)

sten, while the energy deposition calculated per produced neutron remains comparable in both targets. Therefore, a less powerful beam is needed to achieve the same neutron flux in the uranium target as in the tungsten target, and the total energy deposition in both targets [13] remain comparable. Thermal energy released in fission reactions can be converted to electricity and then support, at least in part, the operation of the accelerator.

Apart from the need to build intense neutron sources, using fissile materials in spallation targets opens the possibility to transmute them in fission reactions induced by primary protons and secondary nucleons. Indeed, in addition to unused uranium, each 1000 kg of spent nuclear fuel discharged from a light-water reactor typically contain several kilograms of fissile transuranium elements like plutonium and Minor Actinides (MA): neptunium, americium and curium [14]. Up to 99.9% of plutonium can be extracted and then further used in nuclear reactors [15]. However, other radioactive elements, MA and long-lived fission products, are still very hazardous due to their high radiotoxicity, and their release to environment has to be avoided. There are plans to confine them in very robust vitrified blocks stored in deep geological repositories. Alternatively, MA contained in spent nuclear fuel can be separated and recycled in a dedicated facility operating with fast neutrons (as thermal neutrons are not efficient). As demonstrated by many dedicated studies, see e.g. [14], the extracted MA can be efficiently transmuted into short-lived or stable fission products in fast reactors or in accelerator-driven reactor cores.

Certainly, more theoretical and experimental studies are needed to design an intense fast-neutron source or a spallation target containing fissionable or fissile materials. For many years experimental studies of transmutation of long-lived radiotoxic nuclides have been carried out at the Joint Institute for Nuclear Research in Dubna, Russia, in the framework of an international collaboration [16]. In particular,  $^{237}\text{Np}$  and  $^{241}\text{Am}$  were transmuted into short-lived or stable nuclides by neutrons produced by protons in a thick lead target. Within the project called “Energy plus Transmutation” beams of protons and deuterons were used, and the flux of fast neutrons was amplified by a massive uranium sleeve surrounding a non-fissile target [10, 17, 18].

Detailed theoretical modeling of ADS prototypes should precede their construction and operation. Therefore, a reliable computational tool based on

modern software is necessary to foster studies in the field of the accelerator-driven transmutation. A number of Monte Carlo codes have been used to simulate neutron production and transport in spallation targets of ADS: PHITS [19], SHIELD [20], MCNPX [21] and others. However, to the best of our knowledge, spallation targets containing Am were not studied with these codes so far. In the present work we further develop our Geant4-based code MCADS (Monte Carlo model for Accelerator Driven Systems) [13, 22] in order to apply it for fissile spallation targets containing U and Am. Modeling spallation targets containing americium is motivated by the following two reasons [14]. First, americium is the most abundant MA in spent nuclear fuel and its transmutation into relatively short-lived fission products can reduce the radiotoxicity of radioactive waste by an order of magnitude. Second, the operation of fast reactors with a high content of MA causes certain safety concerns. Alternatively, a subcritical system driven by an accelerator could be a promising option to burn americium extracted from spent nuclear fuel.

## 2. Modeling of americium transmutation by slow and energetic nucleons

As demonstrated in our previous works [13, 22], all physics processes relevant to neutron generation and transport in conventional non-fissile and also in fissionable uranium targets can be successfully simulated with the Geant4 toolkit [23, 24, 25]. In particular, these processes include spallation and fission reactions induced by primary protons and secondary nucleons. Usually specific Geant4 simulations are performed with a set of physical models known as a Physics List. Our MCADS simulations are based on the QGSP\_INCL\_ABLA Physics List proposed by Geant4 developers, which includes the Intra-Nuclear Cascade Liège (INCL) model of version 4.2 coupled with the fission-evaporation model ABLA [26, 27] as core components for our simulations in the considered energy range. Other models involved in this Physics List are described in the Geant4 manuals. The ionization energy loss of charged particles is simulated with standard electromagnetic Physics List of Geant4. As shown in [13], the MCADS model is able to successfully describe experimental data on fission of  $^{238}\text{U}$  by 27 MeV, 63 MeV and 1000 MeV protons. More details on simulations with MCADS can be

found in Ref. [13, 22]. As shown [13], the measured average number of neutrons produced by 400–1500 MeV protons on thick tungsten and uranium targets is accurately reproduced by MCADS using INCLABLA. However, in order to perform simulations with materials containing americium several extensions of the Geant4 toolkit became necessary. This made possible the simulations of proton- and neutron-induced nuclear reactions and elastic scattering of nucleons on Am and other transuranium nuclei [28]. In our recent publication [29] the (p,f), (n,f) and (n, $\gamma$ ) cross sections as well as mass distributions of fission fragments, average number of neutrons per fission event and secondary neutron spectra were calculated with MCADS for  $^{241}\text{Am}$  and  $^{243}\text{Am}$ , and good agreement with experimental data was found. This justifies using MCADS to simulate extended targets containing  $^{241}\text{Am}$  and  $^{243}\text{Am}$ .

The physics of transmutation of  $^{241}\text{Am}$  and  $^{243}\text{Am}$  nuclei by neutron irradiation can be well understood from Fig. 1. Depending on the neutron energy both nuclei can either undergo fission or be transformed via (n, $\gamma$ ) reaction into A+1 isotopes  $^{242}\text{Am}$  and  $^{244}\text{Am}$ . After  $\beta^-$ -decay with half-life times 16 h and 10 h these nuclei change finally into long-lived  $^{242}\text{Cm}$  and  $^{244}\text{Cm}$ , respectively. A sharp rise of the fission cross section at incident neutron energy of  $\sim 0.6$  MeV leads to the dominance of fission of  $^{241}\text{Am}$  and  $^{243}\text{Am}$  over the neutron capture above 1 MeV. Therefore, fast neutrons produced in primary spallation reactions and subsequent neutron-induced fission reactions can be used to burn  $^{241}\text{Am}$  and  $^{243}\text{Am}$  very efficiently.

The radiative neutron capture (n, $\gamma$ ) and fission (n,f) cross sections calculated by MCADS by means of the Monte Carlo modeling of neutron interactions with a thin layer of  $^{241}\text{Am}$  or  $^{243}\text{Am}$  are plotted in Fig. 1 together with the corresponding experimental data [30, 31, 32, 33]. Nuclear reactions induced by neutrons with energy below 20 MeV are simulated by MCADS on the basis of the evaluated nuclear data library JENDL-4.0 [34] converted into a format readable by Geant4 [35]. It was found that the Geant4-compatible nuclear data files based on JENDL-4.0 provide the most accurate description of the energy spectra of secondary neutrons with respect to other nuclear data libraries. The MCADS results below 20 MeV can be compared to the cross sections extracted from ENDF/B-VII.1 [36], which are also shown in Fig. 1. As seen from this figure, a very good agreement is obtained between MCADS,

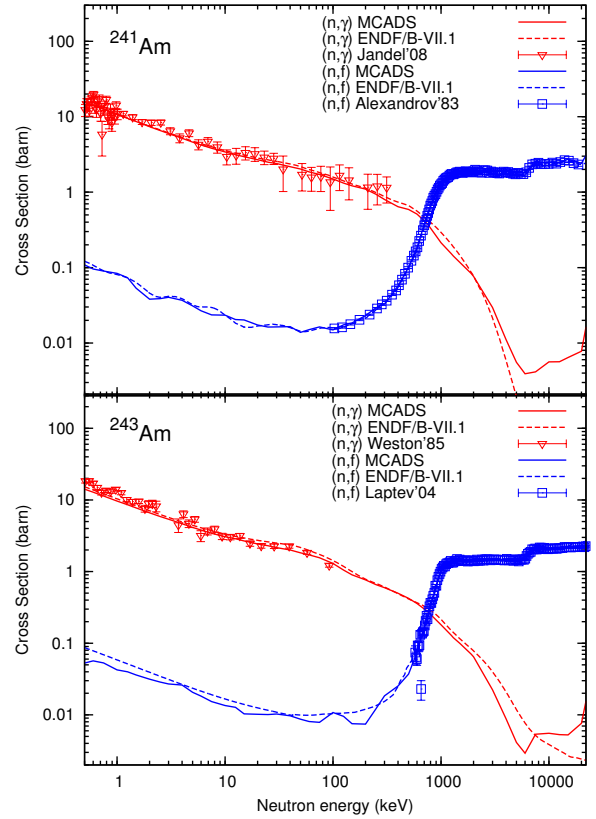


Figure 1: Radiative neutron capture cross section (n, $\gamma$ ), shown in red, and neutron-induced fission cross section (n,f), shown in blue, for  $^{241}\text{Am}$  (top) and  $^{243}\text{Am}$  (bottom) nuclei. MCADS results are represented by solid lines, cross sections from ENDF/B-VII.1 evaluated nuclear data library – by dashed lines. Measured cross sections, (n, $\gamma$ ) for  $^{241}\text{Am}$  and  $^{243}\text{Am}$  from Refs. [30, 31] are shown by triangles, and (n,f) cross section from Refs. [32, 33] – by squares.

experimental data and ENDF/B-VII.1 data.

### 3. MCADS calculations of neutron multiplication in fissile materials

The key issue in designing a spallation target containing fissile materials is the calculation of the neutron multiplication factor to ensure that the target operates in a safe subcritical regime. Neutron multiplication factor  $k$  is calculated with MCADS as the ratio between the numbers of neutrons in the present and previous generations of neutrons averaged over many simulated events. The obvious condition is to keep  $k < 1$ , i.e. strictly in the subcritical mode. The number of neutrons in the target is determined by the balance between their production, absorption and leakage through the target surface.

In order to validate the MCADS model with respect to generation of fission neutrons and their absorption in  $(n,\gamma)$  and  $(n,f)$  processes, we have performed simulations of neutron multiplication in bare (unreflected) spheres made of several fissile materials listed in Table 1. The radius of each sphere made of specific material was gradually increased until  $k$  asymptotically exceeded 1, and the mass of such a sphere was defined as the critical mass for the given material, see Table 1. The critical mass data published by the European Nuclear Society [37] and Monte Carlo simulation results obtained with JENDL-3.2 library for  $^{237}\text{Np}$  and  $^{241}\text{Am}$  in Refs. [38] and [39] are also presented in Table 1. The results of calculations with MCADS for  $^{233,235}\text{U}$ ,  $^{237}\text{Np}$  and  $^{239}\text{Pu}$  agree within 2–8% with the published data [37], but diverge by  $\sim 16\%$  for  $^{241}\text{Am}$ . We attribute this deviations to uncertainties of the nuclear data for  $^{241}\text{Am}$ . As discussed in Ref. [38], the calculated critical mass of  $^{241}\text{Am}$  sphere is very sensitive to the cross sections of neutron-induced reactions tabulated in evaluated nuclear data libraries. The critical mass varies from 55 to 106 kg depending on the nuclear data library used in simulations, while the results obtained with the same library (JENDL-3.2), but with different codes (Polina [38] and MCNP [39]) agree quite well, see Table 1. New measurements and new evaluations of nuclear data for  $^{241}\text{Am}$  are required to reduce these discrepancies. Presently, the lowest estimate of the critical mass of  $^{241}\text{Am}$  ( $\sim 58$  kg) should be considered as a conservative safety limit. Much higher values of the critical mass are reported for  $^{243}\text{Am}$ : from 155.7 to 548.6 kg [38] and from 143 to 284 kg [39], again depending on the data library used in simulations. This indicates the degree of uncertainties in nuclear data available for  $^{243}\text{Am}$ .

Following the validation of MCADS results for the critical mass of the  $^{241}\text{Am}$  sphere without external irradiation, we investigated the criticality issues for a cylindrical spallation target made of pure  $^{241}\text{Am}$  and irradiated by a proton beam. The length of the target was fixed at 150 mm to ensure that all beam protons are stopped in the target material, while the target radii were varied from 40 mm to 110 mm. It was assumed that the target was irradiated by a 600 MeV proton beam with the transverse beam profile of 20 mm FWHM. In Fig. 2 we show the time dependence of the average number of neutrons inside the targets with the target radii of 40, 60, 80, 100, 106 and 110 mm. One can see that the average number of neutrons

in the targets with radii 40–100 mm decreases at late time because less neutrons are produced inside the target volume than escape it or lost in nuclear interactions. The number of neutrons saturates in the target of 106 mm radius (with the weight of 72.4 kg) just 30 ns after the impact of a beam proton. This case is very close to the critical regime with  $k = 0.999$ . Even a smaller fraction of neutrons escape a thicker target of 110 mm radius, and this target becomes supercritical ( $k = 1.013$ ). The corresponding neutron multiplication factors are listed in the legend of Fig. 2.

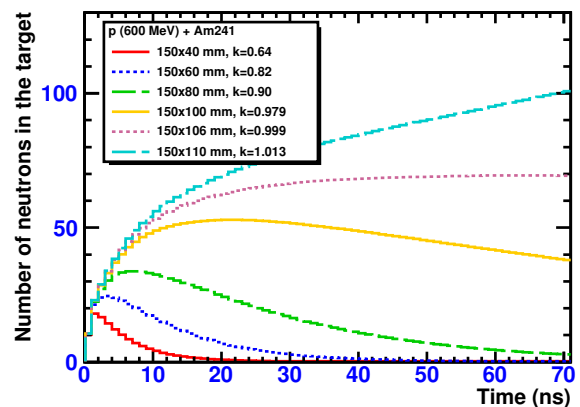


Figure 2: Number of neutrons as a function of time in the cylindrical targets made of  $^{241}\text{Am}$  with the length of 150 mm and various radii and irradiated by 600 MeV protons. The neutron number is normalized per beam particle. The steady-state behavior (horizontal line) corresponds to approaching critical regime with  $k = 0.999$ .

From this criticality study we can conclude that thin cylindrical  $^{241}\text{Am}$  targets with typical radii of  $\sim 50$  mm and length of 150 mm irradiated by 600 MeV protons will operate in a deep subcritical regime with  $k \sim 0.7$ . This suggests that an equivalent amount of  $^{241}\text{Am}$  can be used to build a fissile spallation target. All geometrical configurations of spallation targets containing  $^{241}\text{Am}$  considered below are also designed to operate in a deep-subcritical mode with  $k < 0.6$ .

#### 4. Comparison of targets containing uranium and americium

The operation of spallation targets containing uranium can be simulated with confidence, as the nuclear data for  $^{238}\text{U}$  and all its most abundant

Table 1: Calculated critical masses (kilograms) of bare spheres made of  $^{233,235}\text{U}$ ,  $^{237}\text{Np}$ ,  $^{239}\text{Pu}$  and  $^{241}\text{Am}$ . Data from European Nuclear Society [37] and Monte Carlo modeling results by Polina [38] and MCNP [39] codes both based on JENDL-3.2 library are given for comparison.

Material	MCADS results	data [37]	calculations [38]	calculations [39]
$^{233}\text{U}$	16.1	15.8		
$^{235}\text{U}$	48.4	46.7		
$^{237}\text{Np}$	62.4	63.6	75.0	
$^{239}\text{Pu}$	10.8	10.0		
$^{241}\text{Am}$	66.7	57.6	71.8	73.7

isotopes are reliable in all versions of nuclear data libraries. The simulations of pure uranium targets are very instructive for further comparison with U+Am and pure Am targets. Moreover, the neutrons from U fission can be used for the Am transmutation. Therefore, we have performed simulations of cylindrical targets made of  $^{\text{nat}}\text{U}$ , pure  $^{241}\text{Am}$ , a mixture of  $^{241}\text{Am}$  and  $^{243}\text{Am}$  (57% and 43%, respectively) and americium oxide  $\text{Am}_2\text{O}_3$  with the same isotopic composition of Am. The choice of  $\text{Am}_2\text{O}_3$  is motivated by the fact that americium is usually extracted from spent nuclear fuel in the form of americium oxide. Each target has the radius of 40 mm and length of 120 mm. All these targets have masses well below the critical mass given in Sec. 3. It was assumed that the targets were irradiated by the proton beam with the FWHM of 20 mm and the energy of 600 MeV.

The spatial distributions of neutron flux calculated with MCADS for the considered four targets are shown in Fig. 3. Although the results are given for the proton current of 10 mA, they can be easily rescaled to the actual beam current. The average neutron flux in the americium target ( $1.56 \cdot 10^{16}$  n/s/cm<sup>2</sup>) is higher than in the uranium one ( $1.22 \cdot 10^{16}$  n/s/cm<sup>2</sup>) due to a higher fission cross section for Am. Since the fission cross section on  $^{241}\text{Am}$  is almost 3 times higher than on U, one could expect even a larger difference in favor of  $^{241}\text{Am}$ . However, other reactions, like (n,2n), (n,3n), (n,4n), are much more probable on uranium nuclei. As the result, the difference in the average neutron flux between U and Am targets is reduced. As one can see from Fig. 3, the results for pure  $^{241}\text{Am}$  and mixed  $^{241}\text{Am}+^{243}\text{Am}$  targets are very similar.

Calculated spatial distributions of heat deposition inside the considered targets are presented in Fig. 4. As expected, in fissile spallation targets a significant energy is deposited due to fission re-

actions [22]. The difference between fission cross section on Am and U leads to significantly larger energy deposition in the americium targets (11.9–16.1 MW, depending on the isotope composition) compared to the uranium target (7.7 MW). Therefore, designing a cooling system for the Am target may cause a serious problem.

The values of the average neutron flux ( $1.32 \cdot 10^{16}$  n/s/cm<sup>2</sup>) and heat deposition (11.9 MW) calculated for a pure  $^{243}\text{Am}$  target are lower compared to a pure  $^{241}\text{Am}$  target. This is explained by a lower fission cross section of  $^{243}\text{Am}$  compared to  $^{241}\text{Am}$ , see Fig. 1. The corresponding values for the target made of the mixture of isotopes,  $^{241}\text{Am}+^{243}\text{Am}$ , are intermediate ( $1.44 \cdot 10^{16}$  n/s/cm<sup>2</sup> and 14 MW) with respect to the monoisotopic targets.

It is expected that an increased number of fission reactions in a spallation target makes possible to boost the transmutation rate of americium contained in the target. However, due to the additional energy released in fission events the heat deposition in the target rises too. As seen from Fig. 4, the energy deposition in U and  $^{241}\text{Am}$  targets in the hottest region located close to the target axis exceeds 100 kW/cm<sup>3</sup>, which looks very problematic from technical point of view. Therefore, more sophisticated target systems with a reduced energy deposition per fissioned Am nucleus are needed.

By this reason we extended our calculations for two U targets containing  $^{241}\text{Am}$  as proposed in [13] and a pure  $^{243}\text{Am}$  target mentioned above. Two targets containing  $^{241}\text{Am}$  considered in [13] were schematically designed as following. In the first case  $^{241}\text{Am}$  was uniformly mixed with U with 10% mass concentration and in the second case a cylindrical core ( $V = 200$  cm<sup>3</sup>) of  $^{241}\text{Am}$  is placed in the hottest region of the uranium target. In both cases the target has the radius of 10 cm and length of 20 cm. The heat deposition values per burned Am nucleus in these targets are several times higher

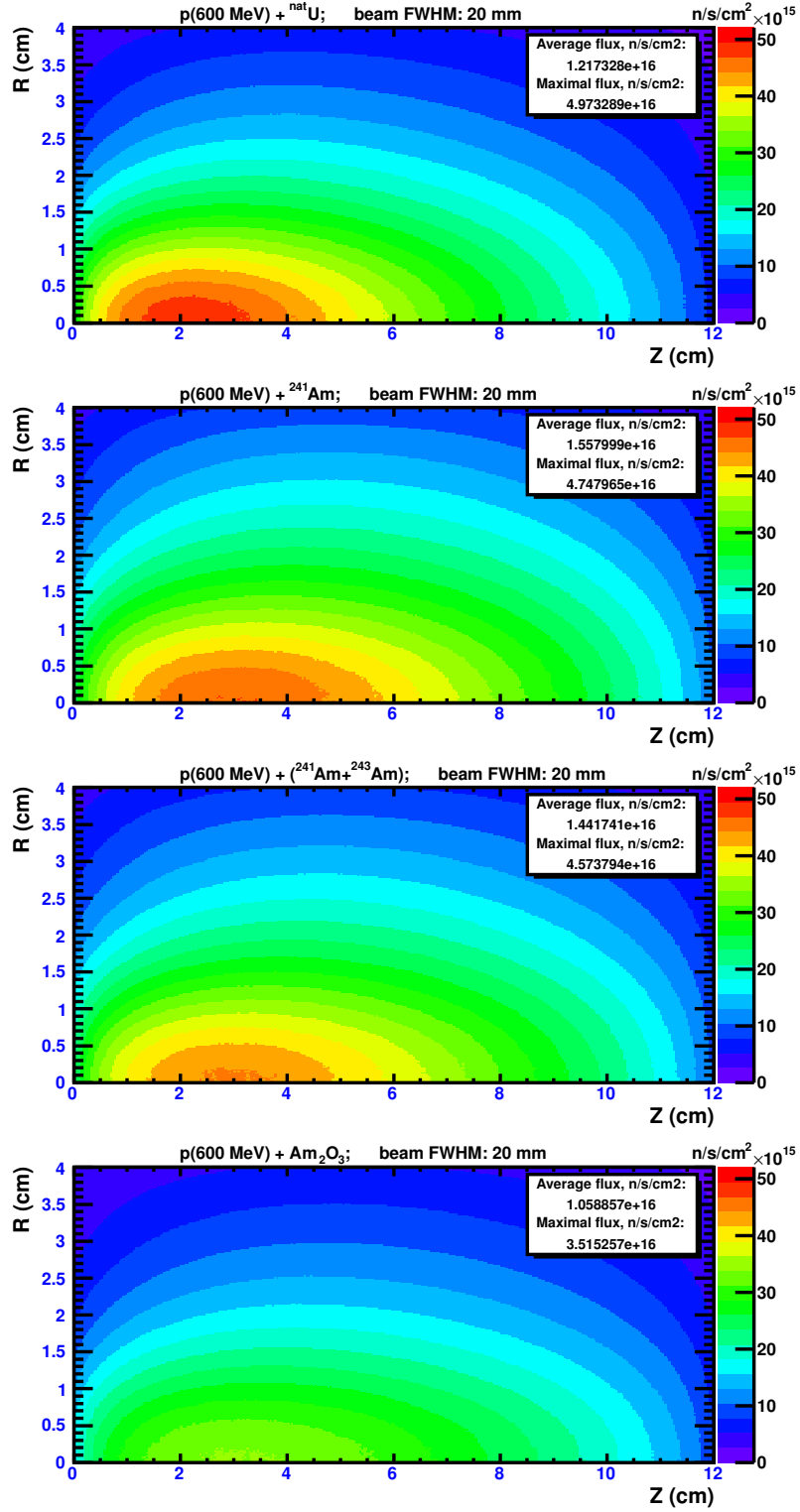


Figure 3: Distribution of the neutron flux inside cylindrical targets made of  ${}^{\text{nat}}\text{U}$ ,  ${}^{241}\text{Am}$ , mixture of  ${}^{241}\text{Am}$  and  ${}^{243}\text{Am}$  and  $\text{Am}_2\text{O}_3$ , all of the same dimensions specified in Table 2. The targets are irradiated by a 10 mA 600 MeV proton beam.

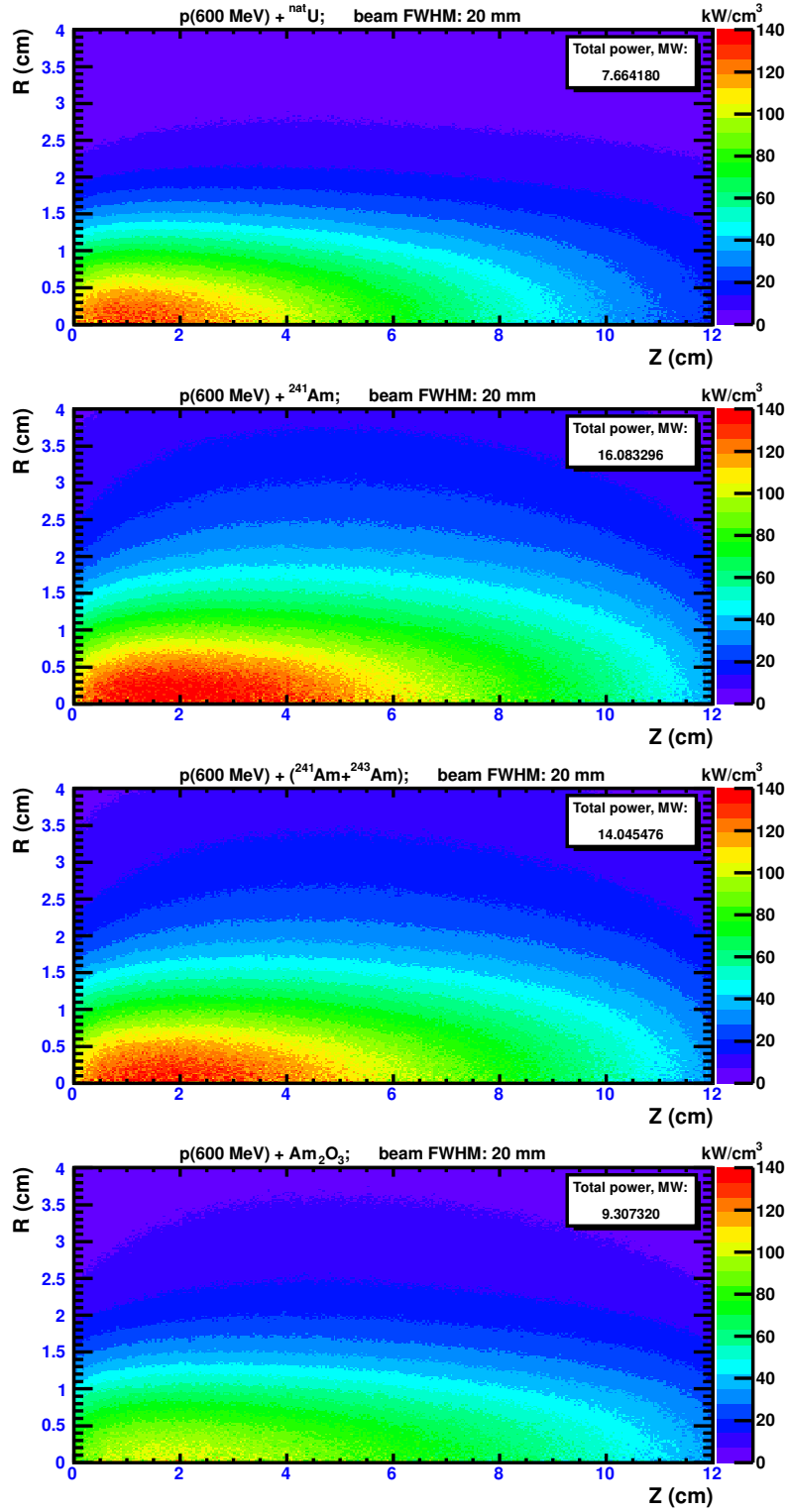


Figure 4: Distribution of heat deposition inside cylindrical targets made of  ${}^{\text{nat}}\text{U}$ ,  ${}^{241}\text{Am}$ , mixture of  ${}^{241}\text{Am}$  and  ${}^{243}\text{Am}$  and  $\text{Am}_2\text{O}_3$ , all of the same dimensions specified in Table 2. The targets are irradiated by 600 MeV proton beam with current of 10 mA.

than the corresponding values for the pure americium targets because of additional fission events of uranium nuclei which also produce neutrons.

The numbers of Am fission events per beam particle  $N_{fis}$  are listed in Table 2 for the six targets containing Am and also for the  $^{nat}\text{U}$  target taken as a reference case, where, accordingly, U fission events are counted. As seen from the table, depending on isotope composition 2 to 3 times more fission events per beam proton are estimated for the pure Am targets compared to the uranium target. Calculated energy deposition per fissioned Am nucleus,  $Q/N_{fis}$ , is also given in Table 2. For the pure Am target this value (203 MeV) is by 30% lower than for the uranium one (279 MeV). As expected, much more energy is deposited per Am fission event in two U+Am targets ( $Q/N_{fis} = 901$  MeV and 793 MeV), because only a part of fission events correspond to Am and most of them to U, according to their concentration in the targets.

Since  $\text{Am}_2\text{O}_3$  target contains less Am nuclei than the pure Am target, this leads to a lower number of fission events and results, correspondingly, in a lower neutron flux ( $1.06 \cdot 10^{16}$  n/s/cm<sup>2</sup>) and lower energy deposition (9.3 MW). The heat deposition per fission event  $Q/N_{fis} = 229$  MeV calculated for  $\text{Am}_2\text{O}_3$  target is close to the  $Q/N_{fis}$  value for the pure  $^{241}\text{Am} + ^{243}\text{Am}$  target.

Finally, burning rates of Am calculated for 10 mA proton beam are presented in Table 2. It was assumed that the burning rates are proportional to the number of Am fission events  $N_{fis}$  in a corresponding target. As found, more than 0.5 kg of  $^{241}\text{Am}$  can be transmuted per month in the spallation target containing exclusively this isotope. Lower burning rates are estimated for other considered geometry and material options, mostly due to a lower Am content. The amount of americium transmuted during the first month of operation  $dm/dt(t=0)$  can be used to calculate the amount of Am burned during the first year. In this estimation it is assumed that the amount of Am  $m(t)$  decreases exponentially,  $m(t) = m_0 \exp(-t/\tau)$ , from its initial amount  $m_0$  with the characteristic time  $\tau = m_0/(dm/dt(t=0))$ . The corresponding results are listed in the last column of Table 2 which gives the minimum annual consumption of Am in the considered spallation targets. Indeed, a possibility to upload additional quantities of Am to the target (e.g. on the regular monthly basis) can be considered, thus substantially increasing the transmutation capability of the ADS system. One can

conclude, that Am can be more efficiently burned in the spallation targets made of pure Am (more than 4 kg of Am per year) compared to mixed U+Am targets. However, the use of larger amounts of pure Am is restricted due to criticality issues.

As shown in our previous publication [13], in the spallation targets made of  $^{nat}\text{U}$  the neutron production is significantly enhanced with respect to the tungsten targets of the same size due to additional contribution of neutron-induced fission of uranium nuclei. In the present study we have found that even more neutrons are produced by fission reactions in targets made of pure  $^{241}\text{Am}$  and  $^{243}\text{Am}$ . This follows from Table 3, where the numbers of neutrons produced or absorbed in various nuclear reactions are given per beam particle for  $^{nat}\text{U}$ ,  $^{241}\text{Am}$  and  $^{243}\text{Am}$  targets of the same size. This means that even small Am targets are highly efficient in incinerating Am in fission reactions. The number of neutrons which escape from the targets are also presented in Table 3. Obviously, the number of leaking neutrons is equal to the difference between the number of produced and absorbed neutrons. The calculations show that about 45% more neutrons are produced in  $^{241}\text{Am}$  target than in  $^{nat}\text{U}$  one. This means that  $^{241}\text{Am}$  target can serve as an intensive neutron source which can be used for various applications.

When dealing with spallation targets made of fissile materials one should consider also an additional heat produced in fission reactions. The total heat deposition  $Q$  and heat per leaked neutron are presented in Table 4 for the same targets as before. One can see that about twice as much heat is generated in the  $^{241}\text{Am}$  target as compared with  $^{nat}\text{U}$  one. This means that a sophisticated cooling system is required for its operation.

## 5. Spallation targets made of Am with U booster and Be reflector

Several advanced geometry options of the spallation target can be considered to increase the burning rate of Am by enhancing the neutron flux inside the target. Two such options are considered below. The first target option (b) consists of an  $^{241}\text{Am}$  cylinder covered by a 2 cm thick  $^{nat}\text{U}$  booster. The second option (c) is additionally covered by a  $^9\text{Be}$  reflector which is 10 cm thick. The core of the both target options consist of a  $^{241}\text{Am}$  cylinder (rod) with the length of 150 mm and radius of 20 mm,



Table 2: Initial amount of Am, number of fission reactions on Am per beam proton,  $N_{fis}$ , heat deposition per fissioned Am nucleus,  $Q/N_{fis}$ , the burning rate of Am at the beginning of operation and the amount of Am transmuted in the first year of operation for various target options.

Material	Length (cm)	Radius (cm)	Initial Am mass (kg)	$N_{fis}$	$Q/N_{fis}$ (MeV)	dm/dt(t = 0) Burning rate (g/month)	Burned in first year (kg)
$^{nat}\text{U}$	12	4	0	2.74*	279*	—	—
$\text{U} + ^{241}\text{Am}$ (10%)	20	10	11.7	1.84	901	120	1.4
$\text{U} + ^{241}\text{Am}$ (core)	20	10	2.68	2.25	739	147	1.6
Pure $^{241}\text{Am}$	12	4	8.24	7.91	203	514	4.3
Pure $^{243}\text{Am}$	12	4	8.24	5.49	216	357	3.4
$^{241}\text{Am} + ^{243}\text{Am}$	12	4	8.24	6.74	208	438	3.9
$\text{Am}_2\text{O}_3$	12	4	6.46	4.07	229	265	2.5

\* Number of fission reactions on U nuclei per beam proton. For all other target options  $N_{fis}$  corresponds exclusively to Am fission events.

Table 3: Average contributions to neutron production and absorption from different reaction channels and the number of leaking neutrons for  $^{nat}\text{U}$ ,  $^{241}\text{Am}$  and  $^{243}\text{Am}$  targets with the length of 12 cm and radius of 4 cm. All numbers are given per beam proton.

	$^{nat}\text{U}$	$^{241}\text{Am}$	$^{243}\text{Am}$
p + A	11.77	9.01	9.34
(n,2n)	0.44	0.04	0.11
(n,3n)	0.15	0.01	0.02
(n,4n)	0.09	0.06	0.06
(n,>4n)	3.80	1.67	1.91
(n,fission)*	4.17	19.54	13.79
produced by other particles	0.15	0.26	0.17
(n, $\gamma$ )	-0.45	-1.45	-1.00
leak	20.12	29.14	24.40

\* Only from neutron-induced fission below 20 MeV.

which is also used alone as a reference target option (a) for comparison. All three target options are schematically shown in Fig. 5 and their parameters are listed in Table 5.

Initially all the three targets contain four times less  $^{241}\text{Am}$  (2.58 kg) compared to the pure  $^{241}\text{Am}$  target considered in Sec. 4. However, the number of fission events per beam proton  $N_{fis}$  in the target (c) is only twice as low as in the target of Sec. 4. This means that Am is burned more efficiently in the presence of the booster, or with both booster and reflector. At the same time  $Q/N_{fis}$  calculated

Table 4: Average heat deposition  $Q$  and heat deposition per leaked neutron  $Q/N$  calculated with MCADS for  $^{nat}\text{U}$ ,  $^{241}\text{Am}$  and  $^{243}\text{Am}$  targets with the length of 12 cm and radius of 4 cm. All values are given per beam proton.

	$^{nat}\text{U}$	$^{241}\text{Am}$	$^{243}\text{Am}$
$Q$ (MeV)	766	1608	1185
$Q/N$ (MeV)	38.1	55.2	48.6

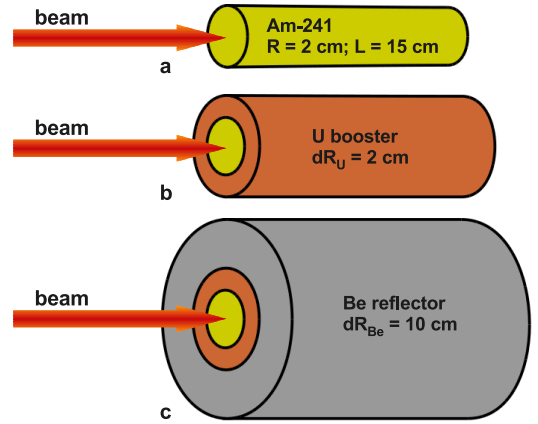


Figure 5: Geometry options: bare  $^{241}\text{Am}$  cylinder (option a),  $^{241}\text{Am}$  cylinder covered by a U booster (option b) and  $^{241}\text{Am}$  cylinder covered by a  $^{nat}\text{U}$  booster and a  $^9\text{Be}$  reflector (option c). The arrows indicate direction of the proton beam.

in the Am core for option (c) is comparable to the same parameter for the pure  $^{241}\text{Am}$  target considered in Sec. 4. The total power deposition in Am

Table 5: Initial amount of Am, number of fission events on Am per beam proton,  $N_{fis}$ , heat deposition per fissioned Am nucleus,  $Q/N_{fis}$ , the burning rate of Am at the beginning of operation and the amount of Am transmuted in the first year of operation for various target options.

Material	Initial Am mass (kg)	$N_{fis}$	$Q/N_{fis}$ (MeV)	dm/dt(t = 0) Burning rate (g/month)	Burned in first year (kg)
$^{241}\text{Am}$ (a)	2.58	3.00	241	194	1.53
$^{241}\text{Am}$ + U booster (b)	2.58	3.79	229	245	1.76
$^{241}\text{Am}$ + U booster + Be reflector (c)	2.58	3.95	228	256	1.79

volume calculated for options (b) and (c) (8.67 and 8.98 MW, respectively) is much less than for the pure  $^{241}\text{Am}$  target (16.08 MW). This indicates the advantages of more complicated target geometries (b) and (c) with respect to simple geometry, since additional neutrons are produced in the U booster. We should also note that no essential improvement in the target performance was achieved by the addition of the Be reflector.

The absolute Am burning rates are smaller ( $\sim 200$  g/month) than for the simple target ( $\sim 500$  g/month). However, the relative burning rates are higher for the advanced options. Indeed, about 42% of the initial Am mass is burned in the first year of ADS operation in the simple pure  $^{241}\text{Am}$  target, as compared with 69% in the advanced target (c).

The distributions of the neutron flux and energy deposition for the options (a)–(c) are shown in Figs. 6 and 7. As seen in these figures, the distributions are more uniform both along the axis of the target and its radius. One can see that adding the booster and the reflector leads to increased average neutron flux by about 50% and 90%, respectively. The highest neutron flux of  $4.89 \cdot 10^{16}$  n/s/cm<sup>2</sup> is reached locally in the target (c) with its average value of  $2.6 \cdot 10^{16}$  n/s/cm<sup>2</sup>. The highest volumetric energy deposition is below 70 kW/cm<sup>3</sup> for the options (b)–(c), which is twice as low as the value of 140 kW/cm<sup>3</sup> calculated for the simple  $^{241}\text{Am}$  target.

## 6. Conclusions

In this paper we have applied the MCADS model based on the Geant4 toolkit for calculating neutron fields and heat deposition in spallation targets containing uranium and americium. We have investigated the criticality of such targets using the Monte

Carlo method. We have demonstrated that the neutron multiplication factor in extended targets containing  $^{241}\text{Am}$  can be reliably evaluated thus allowing the estimation of the critical mass for these fissile spallation targets. The MCADS results for the criticality of targets made of  $^{241}\text{Am}$  provide a guide-line for further studies for their optimization and safe operation in a deep subcritical mode.

Depending on the composition of the target material (pure  $^{241}\text{Am}$ ,  $^{243}\text{Am}$ , their mixture or  $\text{Am}_2\text{O}_3$ ), 2.5–4.3 kg of Am can be transmuted into short-lived or stable fission fragments per year of operation in the spallation target of the ADS facility irradiated by 600 MeV proton beam of 10 mA. The results of simulations with targets of different material composition show that the highest rate of americium incineration is achieved in the targets made of pure americium. As demonstrated by simulations, when Am cylinder is covered by the U booster and shielded by the Be reflector, the relative annual incineration rate of Am increases up to 69%. The burning rate may be increased by  $\sim 50\%$  if uploading of additional quantities of Am to the spallation target is made on a regular basis. Higher incineration rates can be obtained by increasing the neutron multiplication factor up to  $k \sim 0.8$ . However, a high energy deposition in these targets creates serious challenges to their cooling systems. Additional studies of technological issues related to the high heat deposition and also to the radiation damage of target materials due to a very high neutron flux predicted in the target are needed to prove the viability of the proposed concept.

In the uranium targets with small admixture of Am long-lived isotope  $^{237}\text{Np}$  is produced following the capture of two neutrons by  $^{235}\text{U}$  and the subsequent beta-decay. However, our estimations show that the amount of  $^{237}\text{Np}$  produced after a year of irradiation does not exceed 100 grams, which is

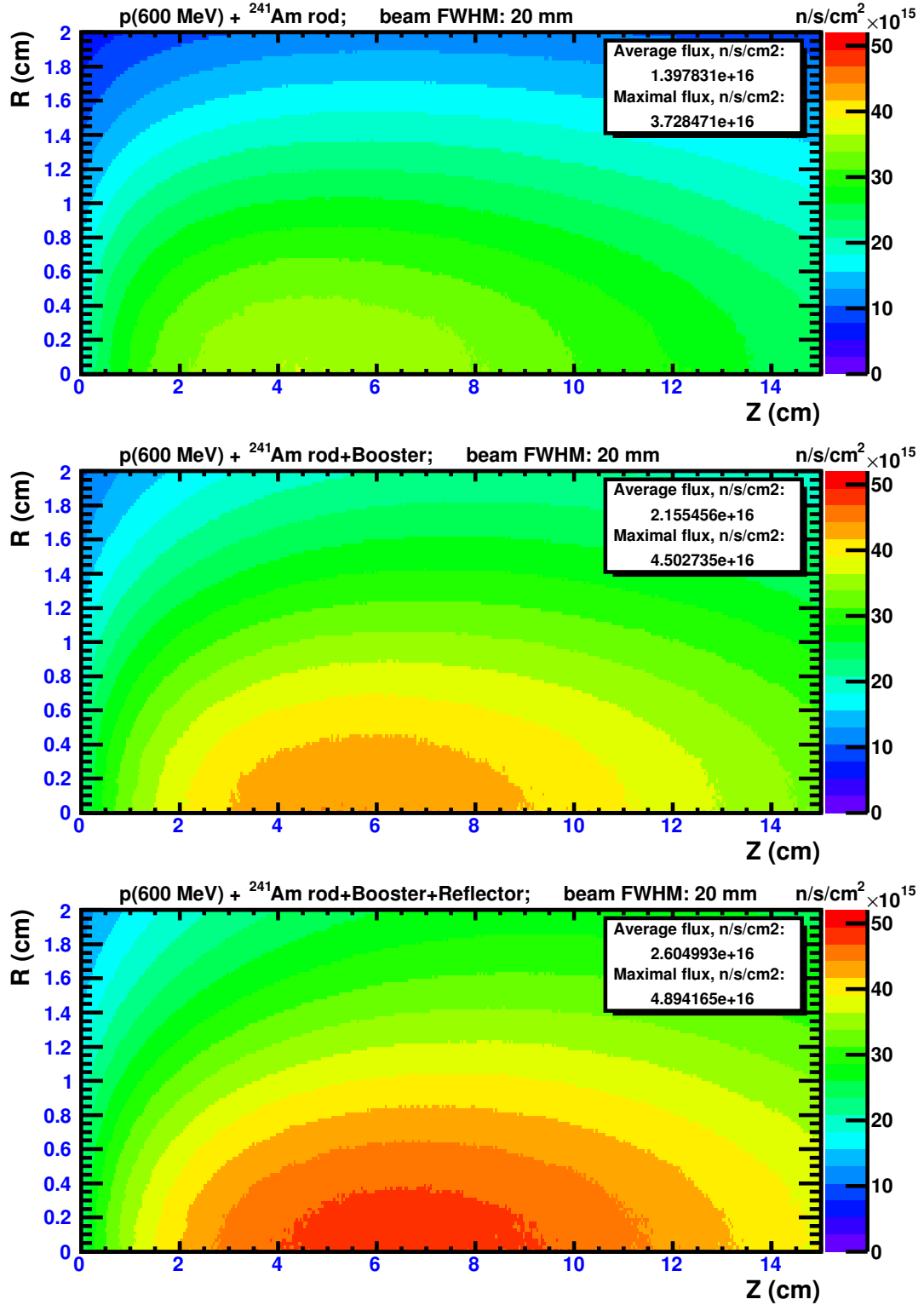


Figure 6: Distribution of neutron flux inside  $^{241}\text{Am}$  cylindrical target (option a),  $^{241}\text{Am}$  cylinder covered by a  $^{235}\text{U}$  booster (option b) and  $^{241}\text{Am}$  cylinder covered by the  $^{235}\text{U}$  booster and a  $^9\text{Be}$  reflector (option c). The distributions are calculated for the targets irradiated by 600 MeV proton beam of 10 mA.

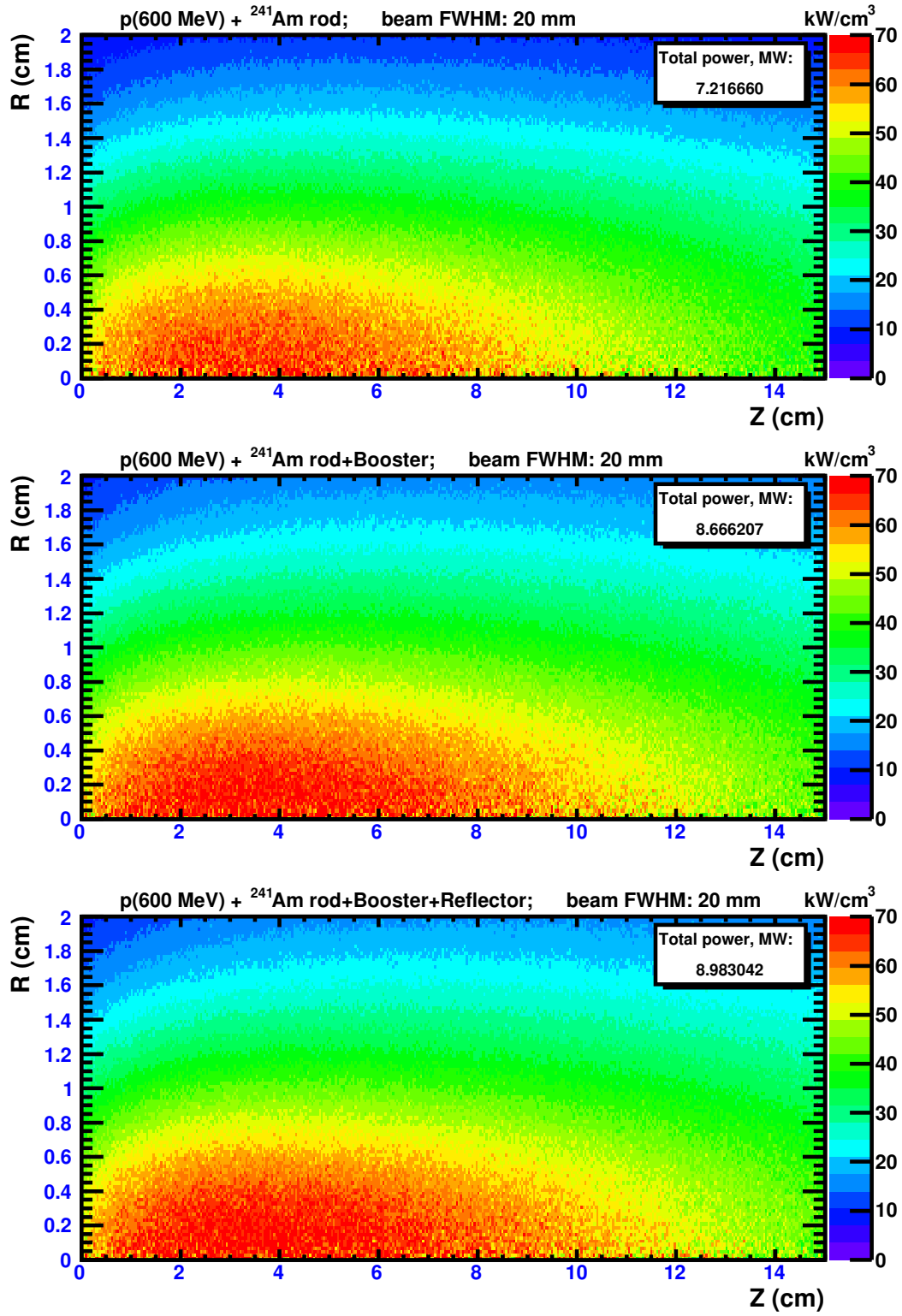


Figure 7: Distribution of heat deposition inside  ${}^{241}\text{Am}$  cylindrical target (option *a*),  ${}^{241}\text{Am}$  cylinder covered by a  ${}^{\text{nat}}\text{U}$  booster (option *b*) and  ${}^{241}\text{Am}$  cylinder covered by the  ${}^{\text{nat}}\text{U}$  booster and a  ${}^9\text{Be}$  reflector (option *c*). The distributions are calculated for the targets irradiated by 600 MeV proton beam of 10 mA.

much less than the mass of transmuted MA. The neutron capture on Am nuclei leading to the production of heavier long-lived MA does not change the total amount of MA in the target.

In this paper we did not discuss a well-known solution where a spallation target of a full-scale ADS facility is surrounded by an extended subcritical reactor core [40, 41]. In this case one could not only use neutrons escaped from the spallation target, but also use additional neutrons produced in the reactor core to burn MA placed there. This may significantly, by a factor of 10 or more, increase the amount of burned MA [40] as compared with burning only in the spallation target. Several such ADS facilities can solve the problem of utilization of MA produced in thermal reactors. The thermal energy produced in the spallation target and reactor core can be converted to electricity in order to cover (at least partially) the energy consumed by the accelerator.

Finally, one can note that the highest neutron flux ( $4.89 \cdot 10^{16}$  n/s/cm<sup>2</sup>) is reached in the target with the booster and reflector, and the average neutron flux ( $2.6 \cdot 10^{16}$  n/s/cm<sup>2</sup>) is also high in this target. Therefore, the ADS facilities can be used to study the properties of materials under the impact of intense irradiation by fast neutrons, as well as for basic research.

## Acknowledgments

Our calculations were performed at the Center for Scientific Computing (CSC) of the Goethe University, Frankfurt am Main. We are grateful to the staff of the Center for support. We thank to E. Mendoza and D. Cano-Ott (CIEMAT, Madrid) for providing the evaluated neutron data in Geant4-format. We are also thankful to Siemens AG for financial support.

## References

## References

- [1] G. S. Bauer, Physics and technology of spallation neutron sources, Nucl. Instrum. Methods Phys. Res., Sect. A 463 (3) (2001) 505 – 543. doi:10.1016/S0168-9002(01)00167-X.
- [2] D. Filges, F. Goldenbaum, Handbook of Spallation Research: Theory, Experiments and Applications, Wiley-VCH Verlag, 2010. doi:10.1002/9783527628865.
- [3] Spallation Neutron Source (SNS) at Oak Ridge National Laboratory (ORNL). URL <http://neutrons.ornl.gov/>

- [4] ISIS pulsed neutron and muon source at the Rutherford Appleton Laboratory in Oxfordshire. URL <http://www.isis.stfc.ac.uk/>
- [5] The ESS project, Vol. III, Technical report and its update, Tech. rep. (2002, 2003).
- [6] M. Arai, K. Crawford, Neutron Imaging and Applications. A Reference for the Imaging Community: Chapter 2. Neutron Sources and Facilities, Springer, 2009.
- [7] A. Herrera-Martinez, Y. Kadi, G. Parks, Transmutation of nuclear waste in accelerator-driven systems: Thermal spectrum, Ann. Nucl. Energy 34 (7) (2007) 550–563. doi:10.1016/j.anucene.2007.02.009.
- [8] A. Herrera-Martinez, Y. Kadi, G. Parks, M. Dahfors, Transmutation of nuclear waste in accelerator-driven systems: Fast spectrum, Ann. Nucl. Energy 34 (7) (2007) 564–578. doi:10.1016/j.anucene.2007.02.008.
- [9] W. Wagner, F. Gröschel, K. Thomsen, H. Heyck, MEGAPIE at SINQ — The first liquid metal target driven by a megawatt class proton beam, J. Nucl. Mater. 377 (1) (2008) 12 – 16. doi:10.1016/j.jnucmat.2008.02.057.
- [10] J. J. Borger, S. R. Hashemi-Nezhad, D. Alexiev, R. Brandt, W. Westmeier, B. Thomauske, M. Kadykov, S. Tiutiunnikov, Fission of <sup>209</sup>Bi, <sup>nat</sup>Pb and <sup>197</sup>Au in the particle field of a fast accelerator driven system, Ann. Nucl. Energy 53 (2013) 50–58. doi:10.1016/j.anucene.2012.07.029.
- [11] S. R. Hashemi-Nezhad, W. Westmeier, M. Zamani-Valasiadou, B. Thomauske, R. Brandt, Optimal ion beam, target type and size for accelerator driven systems: Implications to the associated accelerator power, Ann. Nucl. Energy 38 (5) (2011) 1144–1155. doi:10.1016/j.anucene.2010.12.008.
- [12] J. Galy, J. Magill, H. Van Dam, J. Valko, A neutron booster for spallation sources - application to accelerator driven systems and isotope production, Nucl. Instrum. Methods Phys. Res., Sect. A 485 (3) (2002) 739–752. doi:10.1016/S0168-9002(01)02108-8.
- [13] Y. Malyshev, I. Pshenichnov, I. Mishustin, T. Hughes, O. Heid, W. Greiner, Neutron production and energy deposition in fissile spallation targets studied with Geant4 toolkit, Nucl. Instrum. Methods Phys. Res., Sect. B 289 (2012) 79 – 90. doi:10.1016/j.nimb.2012.07.023.
- [14] M. Salvatores, G. Palmiotti, Radioactive waste partitioning and transmutation within advanced fuel cycles: Achievements and challenges, Prog. Part. Nucl. Phys. 66 (1) (2011) 144–166. doi:10.1016/j.pnpnp.2010.10.001.
- [15] M. Rome, M. Salvatores, J. Mondot, M. Lebars, Plutonium reload experience in French pressurized water reactors, Nucl. Technol. 94 (1) (1991) 87–98.
- [16] W. Westmeier, R. Odoj, S. I. Tyutyunnikov, S. R. Hashemi-Nezhad, W. Ensinger, M. Zamani-Valasiadou, R. Brandt, B. Thomauske, Experiments on transmutation of longlived radioactive waste, ATW International Journal for Nuclear Power 56 (11) (2011) 620.
- [17] J. J. Borger, S. R. Hashemi-Nezhad, D. Alexiev, R. Brandt, W. Westmeier, B. Thomauske, S. Tiutiunnikov, M. Kadykov, V. S. Pronskikh, J. Adam, Studies of the neutron field of the Energy plus Transmutation set-up under 4 GeV deuteron irradiation, Radiat. Meas. 46 (12) (2011) 1765–1769. doi:10.1016/j.radmeas.2011.04.037.
- [18] J. J. Borger, S. R. Hashemi-Nezhad, D. Alexiev,

- R. Brandt, W. Westmeier, B. Thomauske, J. Adam, M. Kadykov, S. Tiutiunnikov, Spatial distribution of thorium fission rate in a fast spallation and fission neutron field: An experimental and Monte Carlo study, *Nucl. Instrum. Methods Phys. Res., Sect. A* 664 (1) (2012) 103–110. doi:10.1016/j.nima.2011.10.027.
- [19] T. Sato, K. Niita, N. Matsuda, S. Hashimoto, Y. Iwamoto, S. Noda, T. Ogawa, H. Iwase, H. Nakashima, T. Fukahori, K. Okumura, T. Kai, S. Chiba, T. Furuta, L. Sihver, Particle and heavy ion transport code system, PHITS, version 2.52, *Journal of Nuclear Science and Technology* 50 (9) (2013) 913–923. doi:10.1080/00223131.2013.814553.
- [20] V. F. Batyaev, M. A. Butko, K. V. Pavlov, A. Y. Titarenko, Y. E. Titarenko, R. S. Tikhonov, S. N. Floriya, B. Y. Sharkov, N. M. Sobolevskii, V. E. Fortov, N. N. Ponomarev-Stepnoi, Analysis of the main nuclear-physical characteristics of the interaction of proton beams with heavy metal targets, *Atomic Energy* 104 (4) (2008) 319–329. doi:10.1007/s10512-008-9035-8.
- [21] G. W. McKinney, Physics and Algorithm Enhancements for a Validated MCNP/X Monte Carlo Simulation Tool, Phase VII, 2012. URL <http://www.osti.gov/scitech/servlets/purl/1046536>
- [22] Y. Malyshkin, I. Pshenichnov, I. Mishustin, W. Greiner, Modeling spallation reactions in tungsten and uranium targets with the Geant4 toolkit, *EPJ Web of Conferences* 21 (2012) 10006. doi:10.1051/epjconf/20122110006.
- [23] S. Agostinelli, et al., Geant4 — A simulation toolkit, *Nucl. Instrum. Methods Phys. Res., Sect. A* 506 (3) (2003) 250 – 303. doi:10.1016/S0168-9002(03)01368-8.
- [24] J. Allison, et al., Geant4 developments and applications, *IEEE Trans. Nucl. Sci.* 53 (1, Part 2) (2006) 270–278. doi:10.1109/TNS.2006.869826.
- [25] J. Apostolakis, et al., Geometry and physics of the Geant4 toolkit for high and medium energy applications, *Radiat. Phys. Chem.* 78 (10) (2009) 859 – 873. doi:10.1016/j.radphyschem.2009.04.026.
- [26] A. Boudard, J. Cugnon, S. Leray, C. Volant, Intranuclear cascade model for a comprehensive description of spallation reaction data, *Phys. Rev. C* 66 (2002) 044615. doi:10.1103/PhysRevC.66.044615.
- [27] A. Heikkinen, P. Kaitaniemi, A. Boudard, Implementation of INCL cascade and ABLA evaporation codes in Geant4, *J. Phys.: Conf. Ser.* 119 (3) (2008) 032024. doi:10.1088/1742-6596/119/3/032024.
- [28] Y. Malyshkin, I. Pshenichnov, I. Mishustin, W. Greiner, Monte carlo modeling of minor actinide burning in fission spallation targets, in: *Proc. Joint International Conference of Supercomputing in Nuclear Applications and Monte Carlo 2013 (SNA+MC 2013)*, 2013.
- [29] Y. Malyshkin, I. Pshenichnov, I. Mishustin, W. Greiner, Interaction of fast neutrons with actinide nuclei studied with Geant4, in: *Proc. International Conference on Nuclear Data for Science and Technology*, New-York, 2013.
- [30] M. Jandel, Neutron capture and neutron-induced fission experiments on Americium isotopes with DANCE, in: *Proc. of the 13th Int. Symp. On Capture Gamma-Ray Spectroscopy and Related Topics*, 2008.
- [31] L. Weston, J. Todd, Neutron-capture cross-section of  $^{243}\text{Am}$ , *Nucl. Sci. Eng.* 91 (4) (1985) 444–450.
- [32] B. Alexandrov, S. Soloviev, P. Soloshenkov, V. Funschstein, S. Khlebnikov, Neutron-induced fission cross section on  $^{241}\text{Am}$ ,  $^{238,240,241}\text{Pu}$ , *Problems of Atomic Science and Technology*, Nuclear Constants 1/50 (1983) 3.
- [33] A. Laptev, A. Donets, V. Dushin, A. Fomichev, A. Fomichev, R. Haight, O. Shcherbakov, S. Soloviev, Y. Tuboltsev, V. A.S., Neutron-induced fission cross sections of  $^{240}\text{Pu}$ ,  $^{243}\text{Am}$ , and  $^{nat}\text{W}$  in the energy range 1–200 MeV, in: *AIP Conference Proceedings*, Vol. 769, 2004, pp. 865–869.
- [34] K. Shibata, O. Iwamoto, T. Nakagawa, N. Iwamoto, A. Ichihara, S. Kunieda, S. Chiba, J. Katakura, N. Otuka, JENDL-4.0: A new library for innovative nuclear energy systems, *J. Korean Phys. Soc.* 59 (2, Part 3) (2011) 1046–1051. doi:10.3938/jkps.59.1046.
- [35] E. Mendoza, D. Cano-Ott, C. Guerrero, R. Capote, New evaluated neutron cross section libraries for the Geant4 code, *Tech. Rep. INDC(NDS)-0612*, International Nuclear Data Committee, IAEA Nuclear Data Section, Vienna, data available online at <http://www-nds.iaea.org/geant4> (2012).
- [36] M. Chadwick, et al., ENDF/B-VII.1 nuclear data for science and technology: Cross sections, covariances, fission product yields and decay data, *Nuclear Data Sheets* 112 (12) (2011) 2887 – 2996. doi:10.1016/j.nds.2011.11.002.
- [37] European nuclear society, <http://www.euronuclear.org>.
- [38] Y. Yudin, Issues of Generation of Neptunium and Americium Isotopes in Nuclear Reactors by Thermal Neutrons and Nonproliferation, ISTC Project 1763p, Technical report for phases C-1 and C-2, *Tech. rep.*, International Science and Technology Center. URL <http://www.partnershipforglobalsecurity.org>
- [39] H. Dias, N. Tancock, C. A., Critical mass calculations for  $^{241}\text{Am}$ ,  $^{242m}\text{Am}$  and  $^{243}\text{Am}$ , in: *The 7th International Conference on Nuclear Criticality Safety (ICNC2003)*, 2003.
- [40] K. Tsujimoto, T. Sasa, K. Nishihara, H. Oigawa, H. Takano, Neutronics design for lead-bismuth cooled accelerator-driven system for transmutation of minor actinide, *J. Nucl. Sci. Technol.* 41 (1) (2004) 21–36. doi:10.3327/jnst.41.21.
- [41] K. Ismailov, M. Saito, H. Sagara, K. Nishihara, Feasibility of uranium spallation target in accelerator-driven system, *Prog. Nucl. Energ.* 53 (7) (2011) 925–929. doi:10.1016/j.pnucene.2011.05.019.